



Faculty of Engineering, Computer and Mathematical Sciences
SCHOOL OF MECHANICAL ENGINEERING

Design of a vibration isolation table with non-contact magnetic springs

PROGRESS REPORT

October 4, 2004

b ll ab sa

Supervisor: Dr Ben Cazzolato
Co-supervisor: Dr Anthony Zander

‘Table that floats on magnets’

Copyright © 2004 Will Robertson

October 4, 2004

School of Mechanical Engineering
University of Adelaide, SA
Australia, 5005

This document has been typeset with the \LaTeX document preparation system using Peter Wilson’s Memoir class.

Page margins have been chosen as a trade-off between achieving the optimal number of characters per line for ease of reading[†], and trying to fit the typeblock onto the poorly-sized (for books), although convenient, A4 stock.[‡] pdf \TeX ’s margin kerning via character protrusion is used to ensure optical straightness of these margins.

PDF hyperlinks have been automatically inserted in all appropriate positions: at footnote, page number, bibliographical, figure, and table references. Furthermore, bibliography entries are appended with page numbers for convenience.

The fonts used in the document are Prof. Hermann Zapf’s *Aldus* at 11 pt for body text, *Palatino* for the titles, and *Euler* for maths. Figure labels are set in Bogusław Jackowski’s *Latin Modern Sans* at various design sizes (based of course on Prof. Don Knuth’s *Computer Modern Sans*). This same font is used on the title page, and the embellished author name is in Hermann Zapf’s *Zapfino*.

[†]Approximately 66.

[‡]For reference, see *The Elements of Typographic Style* by Robert Bringhurst.

Abstract

This document is the eighteen month progress report required for the continuation of the author's Ph. D. candidature in the School of Mechanical Engineering, University of Adelaide. The research aim is to design and build a vibration isolation table using non-contact magnetic springs; the progress of the project is detailed within.

Vibration isolation tables are using in situations that require very precise control of the environment, in which outside disturbances can have a significant detrimental effect (for example, photo-lithography in the semiconductor industry). Commercial isolation tables use pneumatic springs that still transmit vibration at very low frequencies; with non-contact support, it is believed that greater performance may be obtained.

It has been found that non-contact vibration isolation tables, in general, have not yet been built to support large loads. The literature demonstrates using Halbach arrays to increase the flux of magnetic structures; in this work, an analysis of using such arrays in opposition as springs is undertaken, with preliminary research providing some surprising results.

The basic geometry of the proposed magnetic spring design is presented, and shown how it can be adapted to accommodate Halbach arrays in order to increase the load bearing ability of the isolator.

Finally, the details of the equipment to be used for the forthcoming prototype experiments is covered and the testing plan explained.

Table of Contents

1	Introduction	1
1.1	Project exposition	1
1.2	Document structure	2
2	Prior art in the field of magnetic levitation	3
2.1	Levitation techniques	3
2.1.1	Magnetic levitation is impossible!	3
2.1.2	Exceptions to Earnshaw	4
2.2	Non-contact applications of magnetics	6
2.2.1	Magnetic rotary bearings	6
2.2.2	Magnetic couplings	8
2.2.3	Maglev transportation	8
2.2.4	Magnetic actuators	8
2.3	Magnetic arrays	9
2.3.1	Planar arrays	10
2.4	Non-contact magnetic support	10
2.4.1	What is lacking	12
3	Understanding magnets	13
3.1	Sources of the magnetic field	13
3.2	Properties of magnetic flux	15
3.3	Analytic equations	16
3.4	Magnetic materials	18
4	Non-contact magnetic spring design	19
4.1	Requirements of the magnetic design	19
4.2	Simple magnet arrangement	19
4.3	Halbach arrays	22
4.3.1	Planar arrays	22
4.4	Forces between arrays	23
4.4.1	Simple arrays	25
4.4.2	Halbach superposition	25
4.4.3	Cho's array	27
4.4.4	Other array possibilities	28

4.4.5	Arrays for the prototype	29
4.5	Other considerations	29
5	Prototype considerations	32
5.1	Magnets	32
5.2	Forces between magnets	32
5.3	Actuators	34
5.3.1	Prototype electromagnets	34
5.3.2	Actuator placing	35
5.4	Sensors	35
5.4.1	Prototype sensor	36
5.5	Prototypes and testing	36
6	Conclusions	39
6.1	Future work	39

List of Tables

3.1	Typical values for various permanent magnets.	18
5.1	Some appropriate commercial sensors.	36

List of Figures

1.1	Performance of an optical table from Newport.	2
2.1	A ball in unstable equilibrium on a saddle-shaped curve.	4
2.2	Radial bearing cross section.	7
2.3	Two equivalent radial bearings	7
2.4	Backers' magnetic bearing for a rotating shaft.	9
2.5	The magnetic flux lines of a single magnet.	9
2.6	Magnetic flux lines of a Halbach array.	10
2.7	Two planar magnetic arrays shown in the literature.	11
3.1	The magnetic field, \mathbf{B} , both inside and outside a magnet.	14
3.2	The characteristic B vs. H curves for an ideal rare-earth magnet.	15
4.1	Magnets in repulsion create a vertical spring.	19
4.2	'Horizontal' spring.	20
4.3	Spring forces of the vertical & horizontal springs.	21
4.4	Combination vertical/horizontal spring.	21
4.5	Two pairs of facing linear arrays.	22
4.6	Two simple planar magnetic arrays.	23
4.7	Opposing Halbach arrays in the strong and weak fields.	24
4.8	Arbitrary planar array with cuboid magnets.	24
4.9	Forces between three simple facing arrays.	26
4.10	Forces between two planar Halbach arrays.	27
4.11	Cho's array, decomposed into repeating elements.	28
4.12	Two proposed planar arrays with 90° angles of magnetisation.	29
4.13	Conceptual magnetic spring design.	30
4.14	Secondary (outer) magnets may be added to add stability in the rotational direction.	31
5.1	Comparison of analytic and FEA forces.	33
5.2	Performance curves of the radial pole electromagnet.	34
5.3	Calibration for the prototype capacitive sensor.	37
5.4	The prototype magnetic spring (top view).	38
6.1	Approximate timeline for the rest of the project. . .	40

1 Introduction

This chapter introduces the project and describes its aims and its relevance. It concludes with a description of the document structure.

1.1 Project exposition

The purpose of this project is to design and build a vibration isolation table using non-contact magnetic springs. This goal can be split into two: the design of a non-contact magnetic spring (suitable for a vibration isolation table); and the design of the vibration isolation table itself. This document will document the state of the progress toward these goals.

Vibration isolation tables are generally designed to attenuate natural disturbances from the ground to the tabletop. These are used for example in optics systems as well as in situations that involve vibration-sensitive equipment. Current commercial models use pneumatic springs to perform this task, but the degree of isolation they provide at low frequencies is lacking, especially in horizontal degrees of freedom. This is shown in Figure 1.1, which shows the transmissibility curves for the I-500 Series Pneumatic Isolators from Newport.[†] It can be seen that at low frequencies the transmissibility is greater than one—the vibration ‘isolator’ is *increasing* the vibrations at these frequencies. This is because the pneumatic springs transmit low-frequency vibration through their own physical structure. This project is an investigation of the proposal that a non-contact magnetic spring will significantly reduce this unwanted path of vibration transmission and its associated poor vibration isolation.

Since the invention of the rare-earth magnet, there have been great strides in creating wonderful inventions such as the maglev train and the planar levitator. To date, comparatively little work has been undertaken on vibration isolation of large loads using predominantly passive elements. While levitating trains are heavy, they require little positioning accuracy; meanwhile, planar levitators are astonishingly accurate, but may only bear small loads. A vibration isolation table must do both. The few devices reported in the literature thus far are built more for demonstrating advanced control theory in a proof of concept rather than for ap-

[†]<http://www.newport.com/>

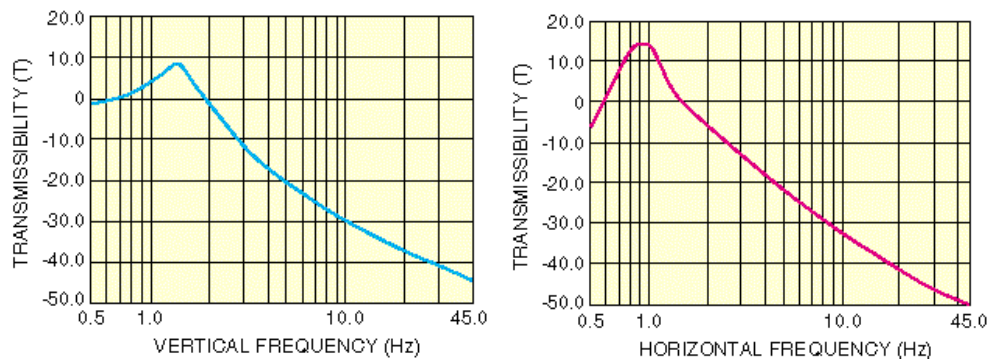


FIGURE 1.1: Performance of an optical table from Newport.

plication. An efficient and scalable magnetic design has thus far been overlooked: this project attempts to rectify the situation.

1.2 Document structure

→ page 19

→ page 32

This concludes the first chapter. The next chapter covers a literature review, followed by some theory on permanent magnets. Chapter 4 describes the design of the magnetic spring, Chapter 5 discusses the production of a prototype. The report concludes with a description of the future work, and of course a list of bibliographic references mentioned to in the text.

2 Prior art in the field of magnetic levitation

With an eye to the practical importance of levitation we feel justified here in disregarding those aspects of it associated with magic, spiritualism, and psychic phenomena...

Boerdijk (1956a)

This chapter is a review of the literature in the field of magnetic levitation. The chapter concludes with the selection of papers that relate specifically to tables that float on magnets.

2.1 Levitation techniques

This section looks directly at those methods of levitation which are in some way electromagnetic in origin; air springs, for example, are not covered, for these systems required a constant supply of compressed air, and furthermore are unable to be used in clean room environments.

2.1.1 Magnetic levitation is impossible!

The act of passively levitating a magnet by another is well known as impossible, although popular unlearned opinion is not aware of the fact. Earnshaw (1842) proved that objects in the influence of fields that apply forces with an inverse-square relation to displacement cannot form configurations of stable levitation. Approximately one hundred years later, Tonks (1940) wrote a paper reminding his contemporaries of the work of Earnshaw by applying the proof specifically to the field of magnetics:

... no flexible assemblage of magnetic poles, in which readjustments in position of the poles in the group can occur, can be stable in either a fixed field or in the field from another such assemblage...

The proof is conceptually quite simple. We start with the equation for the magnetic field; when there are no external current terms, it can be shown to be expressed as Laplace's equation:

$$\nabla \cdot \mathbf{B} = 0 \implies \nabla^2 \mathbf{B} = 0. \quad (2.1)$$

The potential energy of a magnet is proportional to the magnetic field it is subjected to, $U = -\mathbf{M} \cdot \mathbf{B}$, so when the magnetisation is fixed, we have:

$$\nabla^2 U = \frac{d^2 U}{dx^2} + \frac{d^2 U}{dy^2} + \frac{d^2 U}{dz^2} = 0. \quad (2.2)$$

The double differentiations of the energy are the stiffnesses in each direction. But for stable equilibrium, these three terms must be greater than zero. This cannot satisfy Equation (2.2) and thus levitation cannot occur.

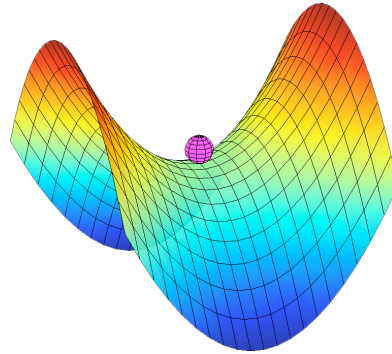


FIGURE 2.1: A ball in unstable equilibrium on a saddle-shaped curve.

This is easy to visualise by analogy. Figure 2.1 shows a ball balancing on a saddle-shaped curve, which we can take to be potential energy of a 2D system. Clearly it is stable in one direction, unstable in the other. Perturbations 'left' or 'right' will result in reaction forces keeping it centred, whereas small displacements 'into' or 'out from' the page will result in increased perturbation.

2.1.2 Exceptions to Earnshaw

Earnshaw's proof does not rule out levitation unconditionally, however. Boerdijk (1956b) reviewed the known methods for levitation, covering levitation by gravitation forces, pressure reaction forces, radiation field forces, and finally in detail, various magnetic and electromagnetic forces.

2.1.2.1 Diamagnetic techniques

Levitations involving diamagnetic material are also exempt from Earnshaw's theorem. This was the motivation for the papers of Boerdijk (1956a,b) in which he cites Braunbek, who derived that magnetic material is governed by Earnshaw's theorem only because it has a relative magnetic permeability (μ_r) greater than one—that is, a permeability greater than that of the surrounding medium. Material with $\mu_r < 1$ is *not* covered by the theorem since the behaviour of the magnetic flux differs, and so static levitation involving magnets and such diamagnetic material is very possible. To demonstrate this, Boerdijk levitated a small cylindrical magnet of dimensions $\varnothing 1 \text{ mm} \times 0.3 \text{ mm}$.

More contemporary studies on diamagnetic levitation look at the levitation of larger objects including strawberries and frogs (Berry and Geim, 1997; Simon and Geim, 2000; Simon *et al.*, 2001), using high-powered electromagnets.

These techniques, however, are not suitable for large load bearing. Even the most diamagnetic substance known, pure bismuth, has $\mu_r \approx 0.9998$ —hardly different than that of air. The forces exchanged via magnetic flux between magnetic and diamagnetic materials, therefore, are incredibly small and not suited at all to the purposes of this research.

Superconducting material, on the other hand, behaves ideally diamagnetic with $\mu_r = 0$, so the forces produced between a superconductor and a magnet are equal to the forces between two permanent magnets themselves. This allows many exciting possibilities for stable levitation. However, such materials must be cooled to very low temperatures with a liquid gas in order to remain superconductive. Such a requirement renders this method financially and functionally impractical for this research. A recent review of the state of the art in this area has been published by Ma *et al.* (2003).

If a material is ever developed that behaves in a super-conductive manner at room temperature, then this research will almost certainly become immediately obsolete. Luckily, there are no indications that this is going to happen in any capacity in the near future.

2.1.2.2 Electromagnetic techniques

Because Earnshaw's theorem looks only at the case for static equilibrium, cases when the magnetic field is dynamic are not covered. This can occur broadly under two circumstances: when the magnetic field is generated with AC currents; and when an unstable permanent magnet arrangement is stabilised with an active control system.

Levitation using a magnetic field produced by AC currents was covered in detail by Laithwaite (1965). The basic mechanism of this type of levitation is that AC currents create dynamic magnetic fields that induce eddy currents in a levitating object, and it is the interaction of the magnetic fields of these induced currents

that causes the levitation. The technique uses a large amount of power, and is not especially suitable for the purposes of this research for this reason.

For an actively stabilised levitation system, the levitation forces are created by permanent magnets (which have DC magnetic fields) and the necessary stabilisation applied with *variable* DC electromagnets with a feedback control system. For this reason the magnetic fields are known as quasi-static. This system was first implemented by Holmes who levitated a magnetic needle, as cited by Boerdijk (1956b). Some more practical examples of these types of system are covered in the next section.

This summary is fairly brief; Bleuler (1992) wrote a more detailed overview. His paper introduces the ‘self-sensing AMB’ (Vischer and Bleuler, 1993) which uses back-electromotive force from the controlling electromagnet to sense the position of the floating element. This eliminates the need for a more classical position sensor (for example, optical or capacitive), but the control system is necessarily more complex and the behaviour not as precise.

2.2 Non-contact applications of magnetics

That magnets can apply forces to one another over a distance is quite a novel concept in a mechanical world accustomed to friction. It has been a short while, relatively speaking, that it has been possible to even *produce* magnets with enough coercive force to apply useful mechanical forces. Non-contact magnetics in mechanical systems is advantageous due to high precision and wear-free operation due to lack of friction. This section looks broadly at some of the main applications of the field.

2.2.1 Magnetic rotary bearings

The oldest dynamic mechanical application of magnetics was for rotary bearings. The classic magnetic bearing supports a shaft by applying radially centring forces on the spinning rotor. An example schematic is shown in Figure 2.2, which is unstable in the axial direction, due to Earnshaw’s theorem. In the most simple of these bearings, this instability is constrained with a physical stop. Backers (1961) developed an early active magnetic bearing which used a control system with DC electromagnets to stabilise the rotor in the unstable axial direction for complete non-contact support.

Yonnet (1978) proved that the forces between radial bearings are equal regardless of whether they are axially magnetised or radially.[†] So, for example, the two bearings shown in Figure 2.3, despite having different magnetisation directions, have the same stiffness (due to the forces being equal).

[†]To be precise, the forces exerted by two magnets upon each other remain equal so long as the sum of their angles of magnetisation remain constant.

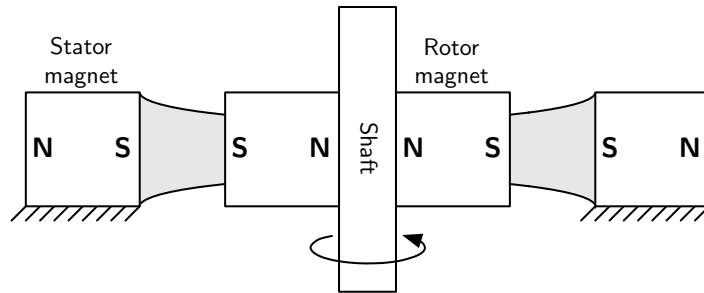


FIGURE 2.2: The cross-section of two radially magnetised ring magnets in a radial bearing.

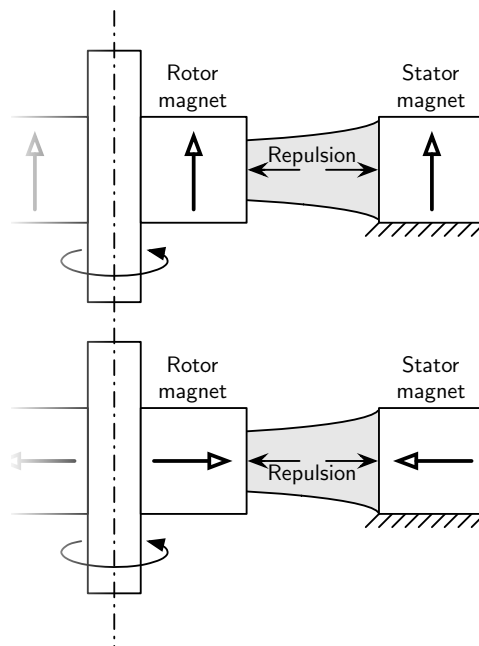


FIGURE 2.3: Two equivalent radial bearings (with equal forces of repulsion), despite their different directions of magnetisation.

His later paper (Yonnet, 1981) continues this work, describing how magnetic bearings may re-arranged to suit different applications, showing every possible simple equivalent axial and radial bearing.

2.2.2 Magnetic couplings

Rotary magnetic bearings have an opposite: the magnetic couple. Rather than isolate components from applied loads, the magnetic couple serves to transmit the forces and couple the two components together. They can be used, for example, to transmit torque between two separate rotating shafts. These are treated by Yonnet (1981), who says periodic recurring magnetisation (see §2.3) is required in order to transmit torque satisfactorily.

2.2.3 Maglev transportation

The largest body of research into magnetic levitation is on so-called ‘maglev’ transportation. Its well-known goal is to use a levitated train or car to provide extremely fast and efficient transportation. This field, which is rather diverse in terms of the techniques under investigation, is finally now achieving commercial application in the real world after some 20 or 30 years of research. While it has some concepts in common with this research (large loads, magnets), the techniques used tend to be rather distanced from those that will be applied for this project because they focus on transportation rather than *elimination* of movement.

2.2.4 Magnetic actuators

In more recent years, another application for magnetic levitation has been investigated, which is the precision control of a levitated platform. Commonly cited for use in the semiconductor industry for photolithography, these levitators were first researched around 20 years ago.

The first designs allowed travel in a single direction, for example, Trumper and Queen (1992), while more recent developments allow more directions of control. Such devices are capable of supporting small loads, and applying horizontal translation forces to effect displacements of up to around 200 mm with nanometre precision. Two planar devices are invented in the independent theses of Kim (1997) and Molenaar (2000). Most recently, a six degree of freedom non-contact actuator was demonstrated by Verma *et al.* (2004).

The reason these devices are unsuitable for this research is due to their travelling capability. Rather than using the primarily magnetic flux for load support, these designs use it in order to provide positioning control in the horizontal directions.

2.3 Magnetic arrays

Backers (1961) developed a theory for magnetic bearings by assuming the effect of curvature of the ring magnets to be negligible and looking at the forces between two large flat plates. He showed that a periodically recurring magnetisation yields stronger forces than a simple homogeneous one. He implements this coarsely in an active magnetic bearing with cross-section shown in Figure 2.4.

It was not until the wide-spread availability of the high energy density rare-earth magnets in the late 1970s that magnetic geometries more complicated than Backers' became feasible. Halbach (1980) pioneered the research on these 'multipole' magnet arrangements, showing how the ideal case of sinusoidal magnetisation may be approximated with a structure made up from discrete magnets as shown in Figure 2.6. This figure shows magnets with 45° increments of magnetisation, but 90° are much more common. In this document, the term 'Halbach array' will refer to the latter form.

In his subsequent paper, Halbach (1981) shows some uses for his multipole magnets; namely, for creating flux patterns for electron beam undulators or wigglers. While his purposes were radically different from those for rotary bearings or this research, he founded the principle that by arranging magnets with rotating magnetisation directions (generally referred to as 'Halbach arrays') the magnetic field is concentrated on one side of the array, and reduced on the other. Figure 2.6 shows this effect with magnetic flux almost exclusively above the array, so the magnetic field strength is much stronger above it than below. Compare this figure to the flux lines of a single magnet as shown in Figure 2.5—notice how in the latter, the flux is symmetrical both above and below the magnet.

Forces between magnets are governed by their field strengths, so it is a natural conclusion that two facing Halbach arrays will have greater forces between them than single magnets of the same size. Yonnet *et al.* (1991) examined this effect relating to the stiffness of rotary bearings. They show that with bearings with 90° rotations between successive magnets (as opposed to Backers's bearing which used 180° increments), the stiffness can be approximately doubled while keeping the magnet volume constant.

Bancel and Lemarquand (1998) look at the field produced by Halbach arrays used for a linear position sensor. Their paper derives equations for the magnetic flux density of an arbitrary magnet, the geometry and magnetisation of which they optimise for their purposes. They then use this equation to compute the effects of a Halbach array (which they plot), but their analytical solutions are not shown. This effort is based around the flux density, so naturally no attempt is made to find the force equations between two arrays.

There have been some very recent papers dealing with the magnetic effects of Halbach arrays used in maglev transportation (Hoburg, 2004), predominantly to ensure that the magnetic field is not strong enough to affect passengers. It is hoped that these analyses will be suitable for describing the magnetic arrangement for this project.

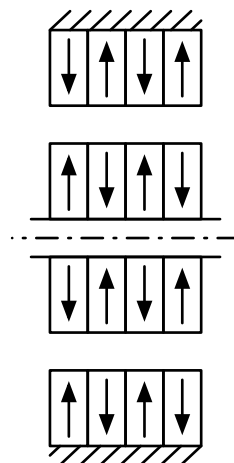


FIGURE 2.4: Backers' magnetic bearing for a rotating shaft.

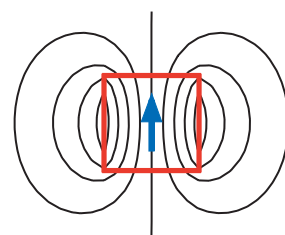


FIGURE 2.5: The magnetic flux lines of a single magnet.

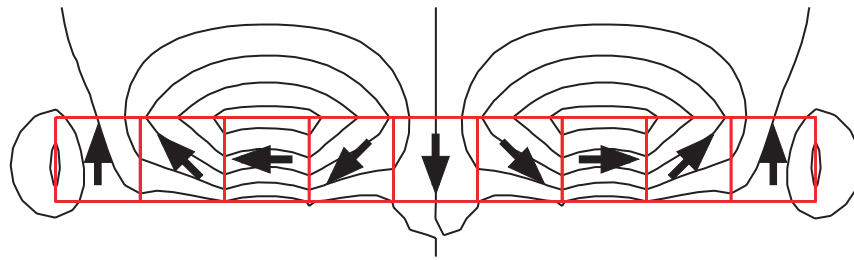


FIGURE 2.6: The magnetic flux lines of a Halbach array made from magnets with 45° magnetisation increments (indicated by the arrowheads). The magnetic field can be seen to be much stronger above the array than below it.

2.3.1 Planar arrays

The previous work covered deals with magnet arrays of constant cross-section. Kim (1997) cites a patent, in which he is involved, that superimposes two orthogonal linear Halbach arrays to create a *planar* structure. Figure 2.7(a) shows the structure, but in his own planar levitator, Kim actually uses a linear Halbach array (later shown in Figure 4.6(b)).

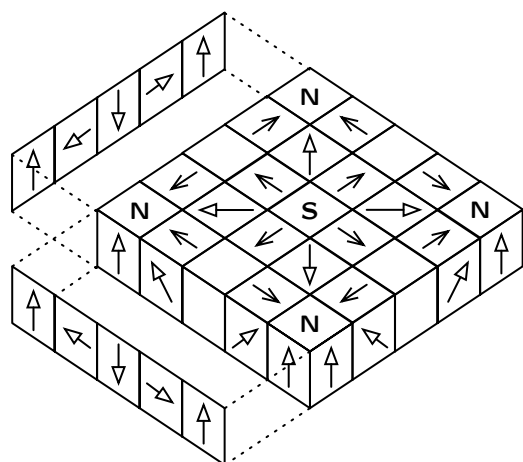
Planar arrays are used quite extensively in the field of planar permanent magnet motors, and there have been some other array configurations developed. Analysis of the magnetic flux produced by various planar arrays, including Kim's, has been done by Cho *et al.* (2001), culminating with the ingenious, superior, design shown in Figure 2.7(b). However, their uses have so far been confined to applications that use the magnetic flux for providing motive force; no analysis has been made on the *forces* between arrays.

2.4 Non-contact magnetic support

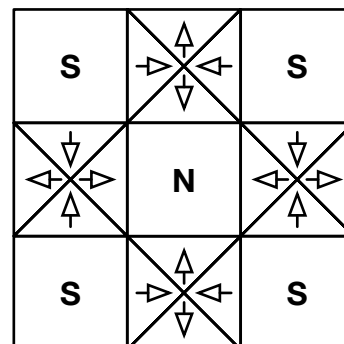
Puppin and Fratello (2002) published a paper that most plainly demonstrates that magnetic springs can be used for vibration isolation, in which the authors make no attempt to achieve contactless suspension—the magnets are horizontally constrained in guides. Furthermore, the springs are only used as passive isolators for vibrations in the vertical direction; no active control is used. Nonetheless, their passive spring was still capable of significant vertical vibration attenuation.

Nagaya *et al.* (1993) constructed a non-contact vibration isolation table; they report a high-stiffness spring with transmissibility approaching zero. Their table used small magnets in a simple design, which could not support large loads. The authors showed later a better control system for their 'perfect noncontact active vibration isolation table' (Nagaya and Ishikawa, 1995)—which refers strictly to the efficiency of their control system and not the load-bearing abilities of the table.

Watanabe *et al.* (1996) wrote a paper detailing a functional vibration isolator using electromagnetic springs, which could support weights of up to 200 kg. The



(a) Planar array created by the superposition of two orthogonal linear Halbach arrays. Non-solid arrow-heads correspond to *diagonal* directions of magnetisation.



(b) The planar array by Cho *et al.* (2001) (top view). Flux travels out of the page from the north- to south-faced magnets, and back through the *array* in the triangular magnets.

FIGURE 2.7: Two planar magnetic arrays shown in the literature.

control system used was quite advanced, utilising a combination of two independent control systems for stable levitation and robust vibration isolation. The magnetic actuator design is not described, however. It is believed that high-powered electromagnets were required for this design; with the current availability of cheap rare-earth magnets, a more efficient design is now possible.

Chang (2001) applied non-linear control to the problem of magnetic levitation, using coupled hybrid magnets (that is, electromagnets biased with permanent magnet cores) that create a magnetic circuit with the levitated table of 20 kg. The paper looks at non-linear analysis and neither passive nor active vibration isolation results are shown.

More recently, Choi *et al.* (2003) have designed a levitation table capable of supporting 15 kg, that is unstable in only one horizontal degree of freedom. However, the magnetic arrangement used for the spring, despite their claims, appears quite unstable and is not suited for scaling up to bear greater loads. Their experiments prove that only a single axis requires control for stability, but the position resolution they achieve is fairly coarse.

A novel design for achieving a theoretically infinite stiffness spring is shown by Mizuno *et al.* (2003a,b). By using physical springs in series with electromagnetic suspension springs, three degrees of freedom of an isolation platform are actively controlled, with the total weight supported around 30 kg. The unstable degree of freedom is in the vertical direction, however, which may prove problematic when increasing the load on the table.

2.4.1 What is lacking

None of these authors have used non-contact forces between magnets to provide a strong passive support. In some cases this is due to a configuration that has the unstable degree of freedom in the same direction as the load bearing. In others it is because strong rare earth magnets were harder to obtain when their research was undertaken. The use of planar magnet arrays for providing supporting forces is not shown in the literature. The aim of this project is to build a non-contact spring with *large* passive load bearing abilities, from the application of such arrays, with the accompanying benefits of non-contact support for vibration isolation.

3 Understanding magnets

3.1 Sources of the magnetic field

Magnetic fields are created by moving electrons. A long straight wire will create cylindrical magnet fields, and a small loop will create a magnetic dipole. Thus, an electron orbiting a proton is the smallest magnetic element. This is a hydrogen atom. In nature, however, hydrogen exists as H_2 , two protons orbited by two electrons—and it happens that the two electrons orbit in opposite directions and the magnetic fields of each cancel each other out. Most material is like this: basically, not magnetic.

The following is a very short introduction to the physics behind magnets. A good reference book which inspired this section is Campbell (1994).

The *magnetic dipole* is designated as the microscopic quantity $\mathbf{m} = i\mathbf{A}$, for a current i and a vector area \mathbf{A} (direction normal to plane). For a collection of magnetic dipoles (as in a permanent magnet), their net effect may be quantified with the macroscopic *magnetisation* of the material, \mathbf{M} :

$$\mathbf{M} = \lim_{\Delta V \rightarrow 0} \frac{\sum \mathbf{m}}{\Delta V}. \quad (3.1)$$

The magnetisation of a permanent magnet creates the magnetic fields that are of such great interest. *Inside* the magnet (with no other external fields present), the magnetic field, \mathbf{B} , is given by the simple relation:

$$\mathbf{B} = \mu_0 \mathbf{M}, \quad (3.2)$$

where μ_0 is the ‘permeability of the vacuum’, an essentially meaningless name given to the necessary constant of proportionality.

So, macroscopic magnetic fields have been derived from microscopic currents. It is possible to take this full circle and now create macroscopic current terms from the magnetic field. The equivalent current density, \mathbf{J}_m around a permanent magnet, created by aligned microscopic orbiting electrons is given by:

$$\mathbf{J}_m = \nabla \times \mathbf{M}. \quad (3.3)$$

This is a good beginning for describing the effects of an *external* current density (\mathbf{J}) acting on the magnet. To separate the effects of induced magnetisation and that

caused spontaneously by magnetic material, a new term is created: the magnetic field strength, \mathbf{H} :

$$\mathbf{J} = \nabla \times \mathbf{H}. \quad (3.4)$$

Now the earlier Equation (3.2) can be adjusted to allow for both internal and external forms of magnetisation (that is, magnetic field caused by permanent magnets or by current carrying conductors). This is the fundamental equation relating the three important terms in magnetics,

$$\mathbf{B} = \mu_0(\mathbf{M} + \mathbf{H}), \quad (3.5)$$

allowing the terms to be unambiguously defined. Henceforth, \mathbf{B} is called the *magnetic flux density*, which is a measure of the total flux per area; and \mathbf{H} is the *magnetic field strength*, the effect of external current sources that creates the magnetic field.[†]

Finally, the *permeability* μ of a material (generally only used when the material is not a permanent magnet) is a varying term describing the ratio between the magnitudes of the \mathbf{B} and \mathbf{H} fields. The *relative permeability* μ_r is the ratio of the permeability to μ_0 .

$$\mu = \frac{B}{H} \quad \mu_r = \frac{\mu}{\mu_0} \quad (3.6)$$

Equation (3.5), may now be used to describe the situation at all points in space. Use Figure 3.1 to note that while inside the magnet, the magnetic field is the vector sum of two components, whereas outside the magnet, the magnetisation is zero and the magnetic field is related to the magnetic field strength by a constant. This results in \mathbf{B} being continuous everywhere, and both \mathbf{M} and \mathbf{H} being discontinuous.

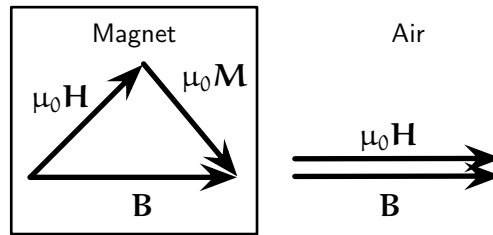


FIGURE 3.1: The magnetic field, \mathbf{B} , both inside and outside a magnet.

This equivalence in air is essentially the reason that there is often confusion between \mathbf{B} and \mathbf{H} . It can be seen that within a magnet, however, their relationship is more complex and important. The performance of a magnet is shown by its \mathbf{B} - \mathbf{H} curve, which is shown for an ideal magnet in Figure 3.2. This curve demonstrates

[†]The names of these terms are not always consistent in the literature. \mathbf{M} is also known as polarisation, and \mathbf{B} and \mathbf{H} are both sometimes known as the magnetic field.

the non-linear and hysteretic effects of the magnetic flux density of a magnetic material as external magnetic field is applied to it.

Two important features are shown in the B-H curve. First, the *remanence* of the magnet, B_r . This value is equal to $\mu_0 \mathbf{M}_{\text{sat}}$ and occurs when there is no external magnetic field. The other is the *coercive force*, H_c , which is the amount of magnetic field strength required to reduce the flux density of the magnet to zero.

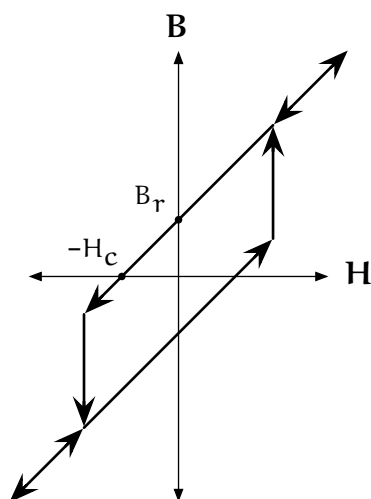


FIGURE 3.2: The characteristic B vs. H curves for an ideal rare-earth magnet.

When the magnet is applying energy, it is operating in the second quadrant of its B-H curve, that is, the section of the curve between the point of remanence and the coercive force, known as the *demagnetisation curve*. This is because the energy used for the demagnetisation is being taken by the causes of the demagnetisation. At some point in this second quadrant, $-\mathbf{B} \times \mathbf{H}$ will have a maximum. Since this is proportional to the energy potential, this is known as the *maximum energy product* $(\mathbf{BH})_{\text{max}}$, and can be shown to be equal in an ideal magnet to:

$$-(\mathbf{BH})_{\text{max}} = \frac{\mathbf{M}_{\text{sat}}}{2} \quad (3.7)$$

The potential energy of the magnet is thus directly related to its magnetisation.

3.2 Properties of magnetic flux

The previous section introduced \mathbf{B} , the magnetic flux density. An analysis of how to derive the paths of magnetic flux is a little beyond the scope of this document, but it is important to discuss the flux lines themselves.

'Magnetic flux' derives its name from archaic models of magnetism, whose proponents believed in the literal flow of a magnetic fluid called the 'luminifer-

ous ether'. Nowadays, scientists tend toward more modern interpretations using electromagnetic fields involving quantum theory. Nonetheless, the name sticks. Magnetic flux, Φ , is therefore defined as the amount of 'fluid' passing through an area:

$$\Phi = \mathbf{B} \cdot \mathbf{A} \quad (3.8)$$

This flux is almost analogous to electric current; the only difference being that electric current is constrained by the conductor it is flowing through, whereas while magnetic flux is known to *prefer* areas of greater permeability, it occasionally can deviate from these simple paths

It is more instructive for a basic understanding of how magnets behave to look at the ways their flux lines interact. The following 'magnet design axioms' are adapted from Moskowitz (1995), whose book covers permanent magnet design for a wide range of uses.

1. Flux lines follow the path of least resistance. This means that they will travel through the shortest path possible, through the material with the *greatest* permeability—so they will travel more readily through magnetic or ferrous material than air, and more readily through air (although only slightly) than diamagnetic material.
2. Flux lines travelling in the same direction repel each other. This means flux lines will never cross.
3. Flux lines enter ferrous material at right angles.
4. Permeability of ferrous material is 'used up' by flowing flux; when the material reaches saturation, flux lines travel as easy though air as through the saturated material.
5. Flux lines travel from North to South poles in closed loops.
6. Magnets are made up of a very large number of unit poles.

From these axioms, one can generate incorrect, yet applicable, theories how and why magnets attract and repel each other. For example, two magnets in repulsion have flux lines opposing each other. It can be imagined that the reason forces occur between them is due to a 'squashing' of the flux lines which the magnets try to oppose—but theories like this only help visualising magnetic behaviour, *not* for explaining the reasons behind it.

3.3 Analytic equations

Following a qualitative discussion of the way magnets behave, it is appropriate to talk about some analytic solutions to the problem. This aspect of the research is

still very much a work-in-progress, for the vector calculus can be fairly involved and for preliminary results, it is quicker to use a finite element analysis. This contrasts with the opinions of the authors from years past, whose computers were not powerful enough to solve complex FEA problems within a reasonable time frame.

Akoun and Yonnet (1984) derived an analytic solution to the problem of two cube magnets with parallel magnetisation. Note that this geometry allows for attraction when the magnetisation direction is in the direction of the offset between the magnets, and repulsion when perpendicular—essentially any configuration is possible.

It is useful to include their equation in the text so that its complexity may be somewhat appreciated.

$$\begin{aligned}
 F_x &= \sum_{i,j,k,l,p,q=0}^1 \left\{ \frac{-J_1 J_2 \phi_x}{4\pi\mu_0} \cdot (-1)^{i+j+k+l+p+q} \right\} \\
 F_y &= \sum_{i,j,k,l,p,q=0}^1 \left\{ \frac{J_1 J_2 \phi_y}{4\pi\mu_0} \cdot (-1)^{i+j+k+l+p+q} \right\} \\
 F_z &= \sum_{i,j,k,l,p,q=0}^1 \left\{ \frac{J_1 J_2 \phi_z}{4\pi\mu_0} \cdot (-1)^{i+j+k+l+p+q} \right\} \quad (3.9)
 \end{aligned}$$

where

$$\begin{aligned}
 \phi_x &= \frac{1}{2} (v^2 - w^2) \ln(r-u) + uv \ln(r-v) + vw \arctan\left(\frac{uv}{rw}\right) + \frac{1}{2} ru \\
 \phi_y &= \frac{1}{2} (u^2 - w^2) \ln(r-v) + uv \ln(r-u) + uw \arctan\left(\frac{uv}{rw}\right) + \frac{1}{2} rv \\
 \phi_z &= -uw \ln(r-u) - vw \ln(r-v) + uv \arctan\left(\frac{uv}{rw}\right) - rw \quad (3.10)
 \end{aligned}$$

and

$$u = \alpha - a(-1)^i + A(-1)^j \quad (3.11)$$

$$v = \beta - b(-1)^k + B(-1)^l \quad (3.12)$$

$$w = \gamma - c(-1)^p + C(-1)^q \quad (3.13)$$

$$r = \sqrt{u^2 + v^2 + w^2} \quad (3.14)$$

For these equations, $2a$, $2b$ and $2c$ are the dimensions of the first magnet; $2A$, $2B$, $2C$ dimensions of the second; α , β , and γ are the distances between their centres.

Furlani (1993) derived similarly complex equations for the exact axial forces between two ring magnets. A different technique that has been used for modelling magnetic forces was shown by Bancel (1999), who introduces the concept of *magnetic nodes*, which may be used to significantly reduce the complexity of the equations of forces between magnets. This technique looks very promising for creating parametrically optimisable equations of force for arbitrary geometries, and it is planned to investigate this method for this project.

3.4 Magnetic materials

There are several materials from which permanent magnets can be made. Short attention will be placed on the cheaper, legacy magnetic materials such as the ferrite magnets and alnico magnets due to their poor performance. Rare-earth neodymium magnets are now quite commonplace and rather cheap, and have much more desirable properties than these old fashioned magnets.

Table 3.1 shows some approximate ranges comparing the properties of the various magnet types available. Clearly, rare earth magnets are capable of much greater energy output, and their high coercivity precludes them from losing their magnetisation through physical impact or proximity with other magnets—unlike the older ferrite and alnico magnets. Their only disadvantage is their low operating temperatures that perhaps will be inconvenient using them for biased, or hybrid, electromagnets, in which a current carrying coil is wrapped around a permanent magnet to increase the output of magnetic field.

Property	Magnet type		
	Ferrite	Alnico	Neodymium
Max. temperature (°C)	400–500	800–900	80–200
Remanence (T)	0.2–0.4	0.5–1.3	1–1.3
Coercivity (kA/m)	100–200	50–160	800–900
Max energy product (kJ/m ³)	6–33	10–80	200–300

TABLE 3.1: Typical values for various permanent magnets. Adapted from information from <http://www.magtech.com.hk/>.

4 Non-contact magnetic spring design

This chapter deals with the geometry of the proposed magnetic spring design.

4.1 Requirements of the magnetic design

The design of the magnetic spring has two broad requirements: firstly, only one degree of freedom instability, because every unstable axis requires actuators for stability control. Therefore it is desired to minimise the number of unstable degrees of freedom in order to minimise the control effort. Furthermore, the unstable direction must be in the horizontal direction for efficient passive vertical load bearing.

Secondly, the magnetic spring design must be scalable to support large loads; the design goal is for the final table to support weight in the order of 10^2 kg. It is desired for the entire weight of the table plus equipment to be supported by the permanent magnets, since weight supported by electromagnets consumes large amounts of power, which is undesirable for numerous reasons, including cost and heat.

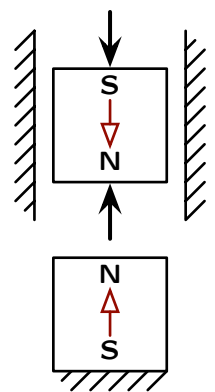


FIGURE 4.1: Magnets in repulsion create a vertical spring.

4.2 Simple magnet arrangement

It is the purpose of this section to ignore the reasons for the magnetic field[†] or any complex equations relating to magnetics, but rather develop an informal understanding of the dynamic behaviour of magnets.

The most simple example of a magnetic spring can be seen in Figure 4.1, with one fixed and one floating magnet arranged vertically. With like poles facing, the two magnets repel each other and produce an air gap between them. Displacement towards each other is restored by the repulsive magnetic force, and displacement away is restored by gravity. The floating magnet must be constrained in both horizontal directions by the shaft. If the constraint is removed, it will be naturally unstable horizontally due to Earnshaw's theorem (see §2.1.1).

A more stable configuration is desired, because the instabilities of this spring occur in two orthogonal horizontal directions. Inspired by the rearrangements of

[†]That is, the underlying quantum mechanical theory that explains electromagnetics.

→ page 3

radial and thrust bearings shown by Yonnet (1981), an improved design is shown in Figure 4.2. Now the spring forces are caused by horizontal magnets in *attraction*, in contrast to the earlier arrangement shown in Figure 4.1 which uses repulsive force.) Two fixed outer magnets both attract a centred floating magnet, so the unstable degree of freedom is in that horizontal direction. Perturbations in the other horizontal direction are restored by the aforementioned attraction, which is similarly the cause of the positive vertical spring stiffness. Note that the diagram works as both a top *and* side view, demonstrating how it is unstable in only one direction.

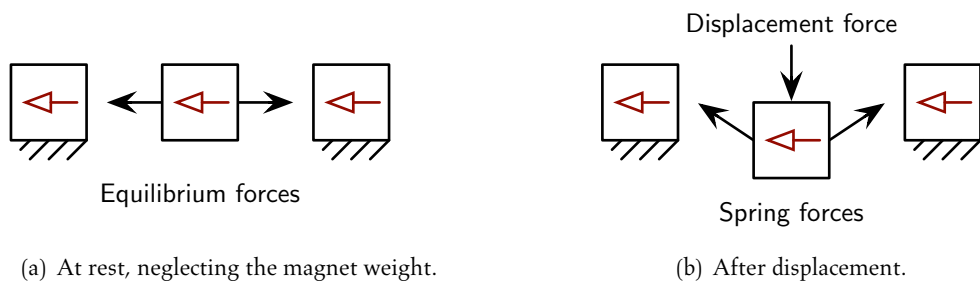


FIGURE 4.2: A 'horizontal' spring with *attracting* magnets to create vertical stiffness, as shown by the reaction forces after displacement.

The removal of an unstable degree of freedom has its consequences, however. The forces between magnetic dipoles are inverse-square functions of the distance between them, and this holds true approximately for magnets as well. In the vertical spring, the effect of increased load on the spring is displacement toward the fixed magnet. This increases the stiffness of the spring.

With the horizontal spring, however, the behaviour is a little more complex. For the case shown in Figure 4.2(a), the only forces on the floating magnet are horizontal. The vertical spring force occurs when the magnet has been displaced as in Figure 4.2(b), which will increase with distance only for a small range. Beyond this, the force will start *decreasing* as the floating magnet becomes further enough away from the fixed magnets—at which point the spring stiffness turns negative and the floating magnet will be unstable.

This parabola effect is shown in Figure 4.3, which also includes the force curve of the vertical spring. The graph was produced from a finite element analysis performed by ANSYS, using half-inch neodymium rare-earth cube magnets.[‡] The effect of varying the gap between the fixed and floating magnets for the horizontal spring is also demonstrated; the further away the fixed magnets are, the weaker the forces are.

Figure 4.4 shows how the two springs discussed so far, horizontal and vertical, may be combined to reap the benefits of both. There are now three fixed mag-

[‡]Remanence $B_r = 1.2\text{ T}$ and coercivity $H_c \approx 900\text{ kA} \cdot \text{m}^{-1}$

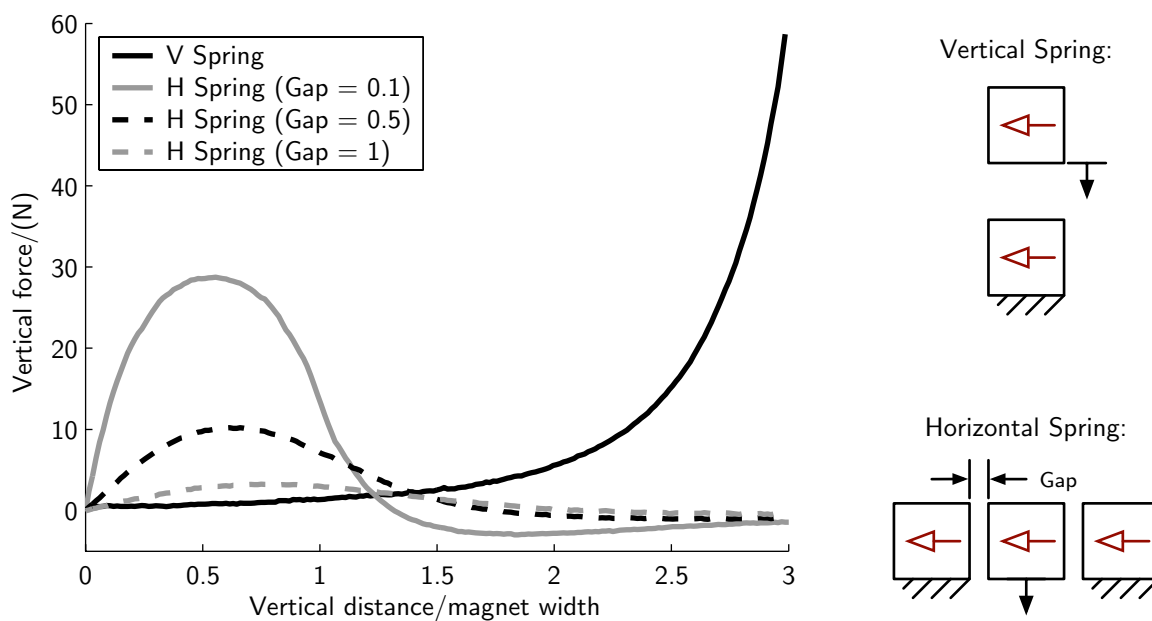


FIGURE 4.3: Forces from FEA comparing the simple vertical and horizontal magnetic springs. The initial gap between the magnets in the vertical spring has been arbitrarily set to 3 magnet widths.

nets: one below, which provides the majority of the stiffness of the spring, and two aside, for stabilising one degree of freedom in the ‘into the page’ direction. This simple design gives a basic framework from which to build up more complex arrangements.

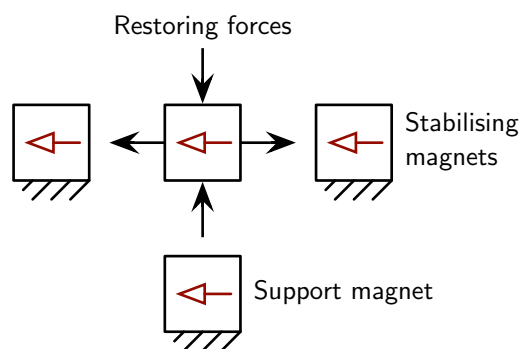


FIGURE 4.4: Combination spring, with the strength of the vertical spring and the stability of the horizontal spring.

4.3 Halbach arrays

→ page 9

The next requirement of the design of the magnetic spring is high load capacity. Since radial magnetic bearings work directly with trying to achieve large forces from arrangements of magnets, it is possible to look to this literature to find prior art. Recall from the literature (see §2.3) that Yonnet *et al.* were able to increase the stiffness of their radial bearing by applying Halbach arrays. They used opposing Halbach arrays, but other configurations are possible.

An examination of the flux lines of various facing Halbach arrays, as shown in Figure 4.5, shows how flux interacts between the two separate linear arrays. It can be seen that simply by varying the direction of magnetisation of the first magnet in the second array, a full sinusoid of forces can be achieved between the arrays—at the limits, total attraction or repulsion in the vertical direction, as demonstrated in figures 4.5(a) and 4.5(b) respectively.

In this configuration, then, this restricts the relative lateral motion to each other that the springs can experience. A slip by two magnet lengths, and the spring will no longer be supporting load—it will be firmly attracted to its former opposer! In practise, this is not a concern. The operation of the spring is design such that free motion is opposed in the lateral directions, and will be implemented with a physical stop (only at the extremes of displacement so as to remain non-contact, of course) to prevent calamity of this sort.

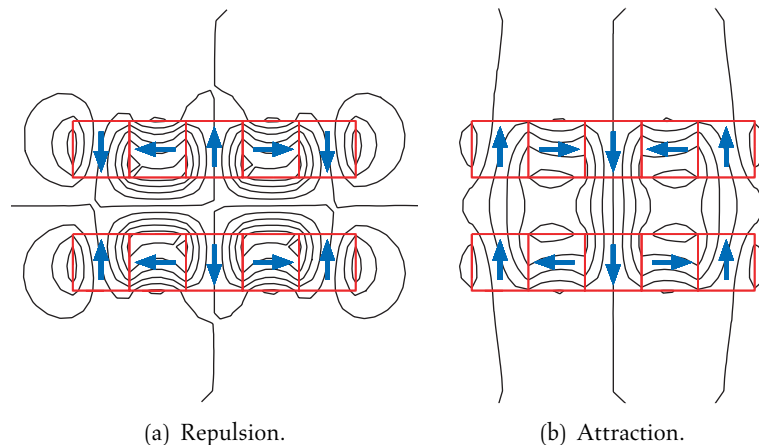


FIGURE 4.5: Two pairs of facing linear arrays.

4.3.1 Planar arrays

The author is unaware of any attempt to use Halbach arrays to increase the stiffness of linear magnetic springs. The literature shows planar arrays developed for

flux linkage for reluctance actuators, not for generating force; a notable separation exists here.

The ‘patchwork’ array shown in Figure 4.6(a) is the most simple. See Hinds cited by Kim (1997), or Chitayat cited by Cho *et al.* (2001) for its use in other circumstances. The array used by Kim is shown in Figure 4.6(b), despite the fact that he demonstrated the Halbach superposition as shown in §2.3.

→ page 9

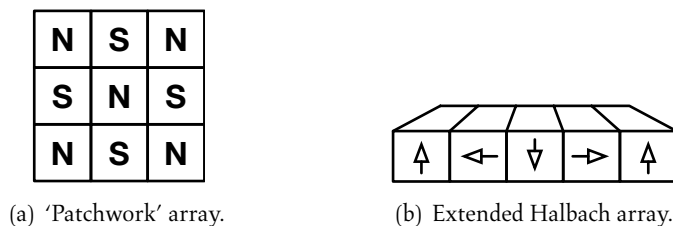


FIGURE 4.6: Two simple planar magnetic arrays: (a) shows the planar analogue to Backers’ arrangement; (b) is a Halbach array extended into a planar structure.

4.4 Forces between arrays

It has been previously mentioned that the purpose of the arrays is to focus the flux into the areas where it will be generating spring force. This has the beneficial side-effect of reducing the forces created between an array and any ferrous or magnetic object that is nearby in any other direction. Figure 4.7 shows three Halbach arrays. They are arranged all in repulsion, but the top two have their strong sides facing whereas the bottom two have their weak sides facing. In this static arrangement, the forces between the strong pair are about 200 times stronger than the weak pair. This demonstrates the advantages of using Halbach arrays in this manner.

As previously mentioned, Cho *et al.* (2001) derived analytic equations for the flux above the patchwork and extended linear array designs from Figure 4.6, and Kim’s Halbach superposition from Figure 2.7(a). An analytical solution for their own array is not attempted, due to the complexity of the model (it is assumed).

→ page 11

However, it is as complex again to derive the forces between two such facing arrays. Therefore, analysis is performed with finite element analysis in ANSYS. For this purpose, then, the only relations required are equations deriving the magnetisations of each individual magnet. Figure 4.8 shows an arbitrary planar array, created from a number of equal-sized cuboid magnets stacked perpendicular to the \hat{z} direction, for which we define the magnetisation, \mathbf{M} , of *each* magnet as:

$$\mathbf{M}(i, j) = M_x \hat{x} + M_y \hat{y} + M_z \hat{z} \quad (4.1)$$

where i and j are the magnet numbers in the \hat{x} and \hat{y} directions, respectively. This equation is redefined to remove the constant magnetisation magnitude, M , from

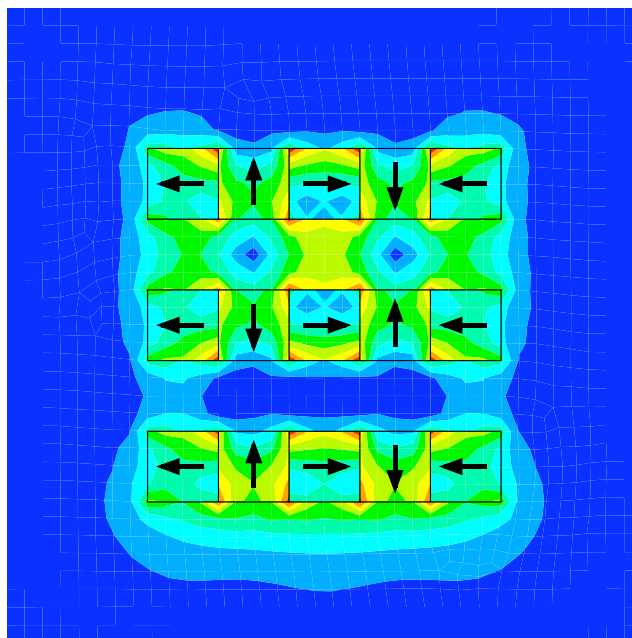


FIGURE 4.7: Opposing Halbach arrays in the strong and weak fields.

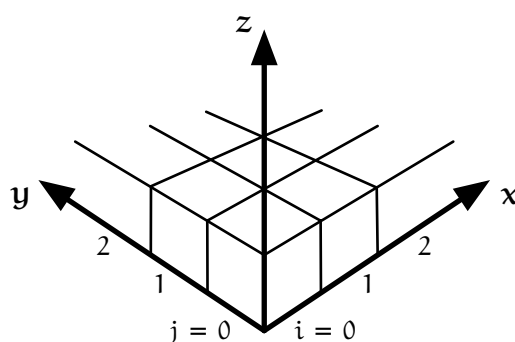


FIGURE 4.8: Arbitrary planar array with cuboid magnets. i and j are the magnet numbers in the x and y directions.

each term:

$$\mathbf{M}(i, j) = M \cdot \hat{\mathbf{M}}(i, j) \quad (4.2)$$

$$\text{where } \hat{\mathbf{M}}(i, j) = \hat{M}_x \hat{\mathbf{x}} + \hat{M}_y \hat{\mathbf{y}} + \hat{M}_z \hat{\mathbf{z}} \quad (4.3)$$

Note that this is the magnetisation of only the bottom array; the magnetisation of the opposite, repulsive, array can be generated by inverting the magnetisation in the facing direction: $\hat{M}_{z_2} = -\hat{M}_z$.

4.4.1 Simple arrays

To begin, the simple arrays are examined and the vertical forces between two facing arrays solved statically for a range of displacements.

For opposing homogeneous arrays, equivalent to a single magnet, the magnetisations do not vary:

$$\hat{\mathbf{M}} = (0, 0, 1). \quad (4.4)$$

For simple 'patchwork' magnet arrangement as in Figure 4.6(a), the magnetisation directions are:

→ page 23

$$\begin{aligned} \hat{M}_x &= 0, \\ \hat{M}_y &= 0, \\ \hat{M}_z &= \cos(i\pi) \cos(j\pi). \end{aligned} \quad (4.5)$$

For the case when the linear Halbach array (with 90° rotations) is extended into the third dimension as in Figure 4.6(b), the magnetisation of the array is:

→ page 23

$$\begin{aligned} \hat{M}_x &= \cos\left(\frac{1}{2}i\pi\right), \\ \hat{M}_y &= 0, \\ \hat{M}_z &= \sin\left(\frac{1}{2}i\pi\right). \end{aligned} \quad (4.6)$$

The forces between facing pairs of these three arrays is shown in Figure 4.9. For this graph, and subsequent ones, 5 × 5 arrays of half-inch rare-earth cube magnets have been used. Surprisingly, the patchwork array did not perform better than the homogeneous array except in close proximity. The finite element analysis in ANSYS was capable of generating solutions for distances equal to 0.3 magnet widths between the arrays; closer than this and the number of nodes required for the solution surpassed the capacity of the department's license for the software.

4.4.2 Halbach superposition

The array developed by Kim is shown in Figure 2.7(a). The magnetisation can be

→ page 11

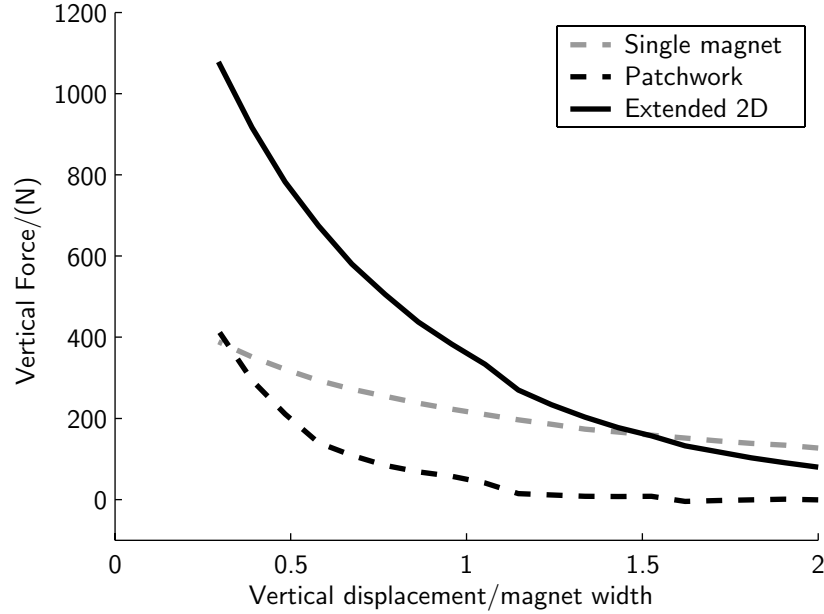


FIGURE 4.9: Forces between three simple facing arrays.

given in two ways. A strict superposition, as performed by Kim, would simply add the magnetisations of two orthogonal Halbach arrays, yielding:

$$\begin{aligned}
 \hat{M}_x &= -\sin\left(\frac{1}{2}i\pi\right), \\
 \hat{M}_y &= -\sin\left(\frac{1}{2}j\pi\right), \\
 \hat{M}_z &= \cos\left(\frac{1}{2}i\pi\right) + \cos\left(\frac{1}{2}j\pi\right).
 \end{aligned} \tag{4.7}$$

However, an inspection of the magnetisations shows that the magnets are now significantly stronger than for the other arrays that have been looked at. This is not particularly convenient for comparing array performance. To make a comparison worthwhile, some care must be taken to ensure the normalised magnetisations of each block are equal and within the same range ($0 \leq \hat{M}_{x,y,z} \leq 1$) as the other arrays already shown:

$$\begin{aligned}
 \hat{M}_x &= -\frac{1}{\sqrt{2}} \sin\left(\frac{1}{2}i\pi\right), \\
 \hat{M}_y &= -\frac{1}{\sqrt{2}} \sin\left(\frac{1}{2}j\pi\right), \\
 \hat{M}_z &= \frac{1}{\sqrt{2}} \sqrt{\cos^2\left(\frac{1}{2}i\pi\right) + \cos^2\left(\frac{1}{2}j\pi\right)}.
 \end{aligned} \tag{4.8}$$

The first array will be referred to as a ‘Halbach addition’, whereas the second will be called a ‘Halbach superposition’. Figure 4.10 demonstrates the significant differences between the two, showing the forces with the extended Halbach array (refer to Equation (4.6)) for comparison. The simple addition of two orthogonal arrays

shows approximately double the spring stiffness—consistent with the method of generation. However, facing superposition arrays creates approximately *half* the force as between the simple extended Halbach arrays. This is surprising, and yet promising, since the magnetisations for this planar array are awkward to obtain.

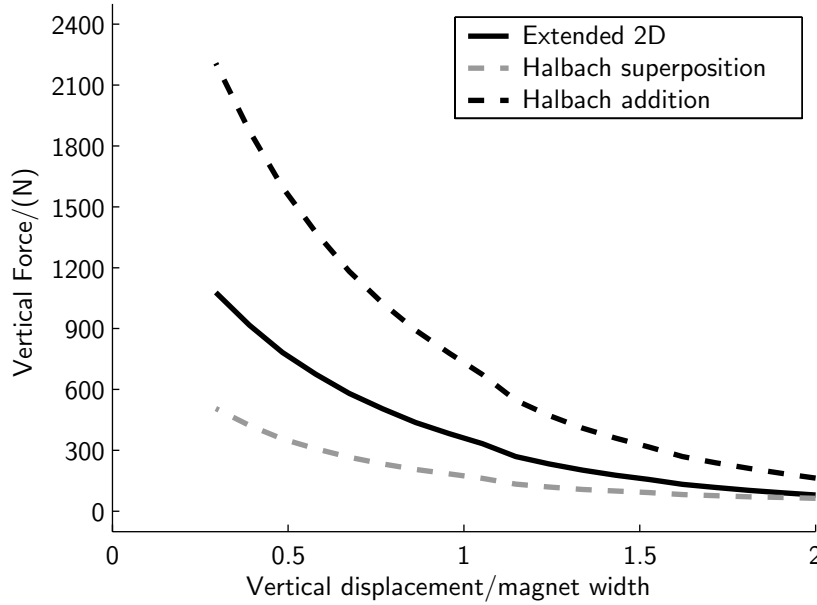


FIGURE 4.10: Forces between planar arrays: Halbach addition and Halbach superposition.

4.4.3 Cho's array

To look at the aforementioned array by Cho *et al.* (2001), a more complex model is required than the arbitrary array composed of simple block magnets. For this task, each block magnet may be decomposed into triangular cross-section pieces, as shown in Figure 4.11. The magnetisations can then be expressed in terms of \mathbf{M}_H , those square blocks containing multipole magnetisations in the \hat{x} - \hat{y} plane, and \mathbf{M}_V , those in the \hat{z} directions, as shown in the figure: (note that $\frac{1}{2}(1 - (-1)^i) = 0, 1, 0, 1, \dots$)

$$\begin{aligned} \hat{\mathbf{M}}_{i,j} = & \frac{1}{4}(1 - (-1)^j) \left(\hat{\mathbf{M}}_V(1 - (-1)^i) - \hat{\mathbf{M}}_H(1 - (-1)^{i+1}) \right) \\ & + \frac{1}{4}(1 - (-1)^{j+1}) \left(\hat{\mathbf{M}}_H(1 - (-1)^i) - \hat{\mathbf{M}}_V(1 - (-1)^{i+1}) \right) \end{aligned} \quad (4.9)$$

where

$$\hat{\mathbf{M}}_V = (0, 0, 1), \quad (\text{for } k = 0, \dots, 3) \quad (4.10)$$

$$\hat{M}_{H_x} = \cos\left(\frac{1}{2}k\pi\right),$$

$$\hat{M}_{H_y} = \sin\left(\frac{1}{2}k\pi\right),$$

$$\hat{M}_{H_z} = 0. \quad (4.11)$$

→ page 11

It may be helpful to refer to Figure 2.7(b) which shows the full magnetisation directions for the triangular blocks. Force analysis is yet to be performed comparing this array to the others.

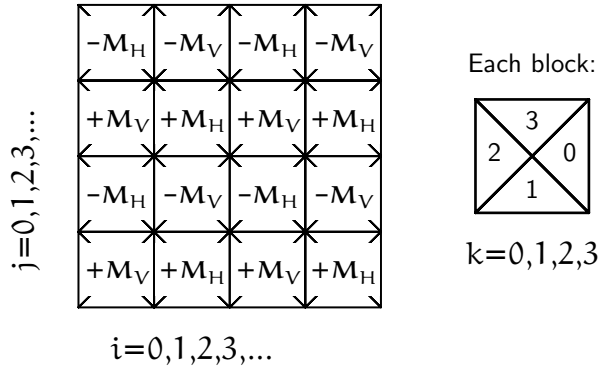


FIGURE 4.11: Cho's array, decomposed into repeating elements.

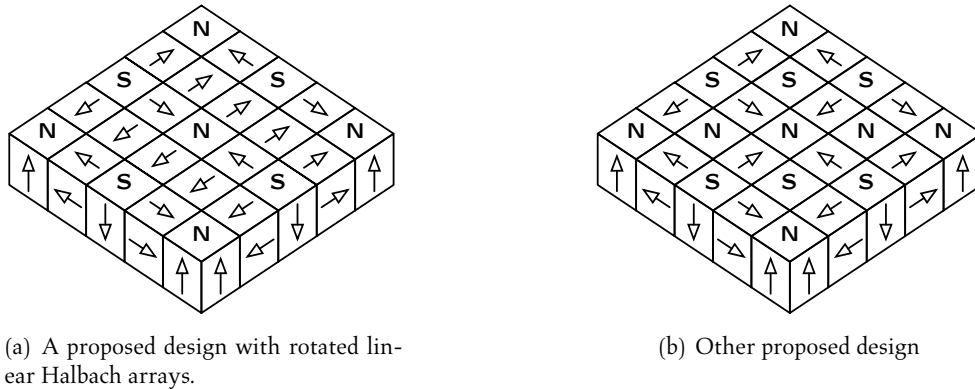
4.4.4 Other array possibilities

The disadvantage of Cho *et al.*'s and Kim's planar arrays is that they use very irregular magnets. It is proposed that an array with similar capabilities can be constructed only using cube magnets with 90° directions of magnetisation. Diagrams are shown in Figure 4.12.

The first design, Figure 4.12(a) uses rotated linear arrays of cube magnets following the same pattern as a Halbach array takes for single magnets. The magnetisation directions are:

$$\begin{aligned} \hat{M}_x &= \cos\left(\frac{1}{2}i\pi\right) \sin\left(\frac{1}{2}j\pi\right), \\ \hat{M}_y &= \sin\left(\frac{1}{2}i\pi\right) \cos\left(\frac{1}{2}j\pi\right), \\ \hat{M}_z &= \cos\left(\frac{1}{2}i\pi\right) - \sin\left(\frac{1}{2}j\pi\right). \end{aligned} \quad (4.12)$$

The second design, Figure 4.12(b), was developed by extending two Halbach arrays in orthogonal directions starting from an initial magnet and filling in the



(a) A proposed design with rotated linear Halbach arrays.

(b) Other proposed design

FIGURE 4.12: Two proposed planar arrays with 90° angles of magnetisation.

gaps. The magnetisation directions are:

$$\begin{aligned}\hat{M}_x &= \cos\left(\frac{1}{2}i\pi\right) \sin\left(\frac{1}{2}j\pi\right), \\ \hat{M}_y &= \sin\left(\frac{1}{2}i\pi\right) \cos\left(\frac{1}{2}j\pi\right), \\ \hat{M}_z &= \cos\left(\frac{1}{2}i\pi + \frac{1}{2}j\pi\right).\end{aligned}\quad (4.13)$$

Finite element modelling is still in progress, but initial results indicate that these two conceptual designs show less promise than the extended linear array. However, there are a number of other designs that could be proposed in this manner, including one based on Cho's array, which still require consideration.

4.4.5 Arrays for the prototype

The use of magnet arrays is advantageous to two areas of the prototype magnetic spring: firstly, for the magnets which provide the main spring forces; and secondly for the magnets which help stabilise the spring with horizontal forces. Theoretical results indicate that the use of linear magnet arrays maximises these forces.

The geometry of the design lends itself towards using linear arrays for the stabilising magnets and a planar array for the support magnets, such as shown in Figure 4.13. In this way, the flux created by the permanent magnets will be entirely used for the forces on the spring.

4.5 Other considerations

This section contains some musings on the eventual design of the non-contact table. In the design discussed, there has been no mention of a possible rotational instability that will occur due to the multitude of positions where translational instability occurs. This case may be compared to the bearing with ring magnets which is similarly rotationally unstable in a radial bearing configuration.

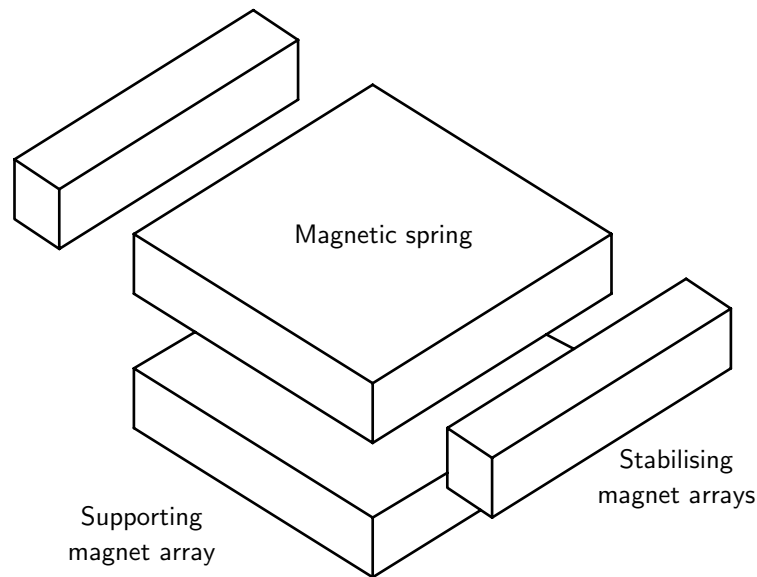


FIGURE 4.13: Conceptual magnetic spring design.

Delamare *et al.* (1994) look at this problem and manage to remove the rotational instability by adding a weaker, *axial* bearing to the system—that is, opposite in effect to the main aims of the system. The coupling of the axial and radial bearings eliminates the rotational instability, but the strength of the radial bearing overpowers the axial bearing for normal operation.

This is more easily explained with a diagram. Figure 4.14 shows how this idea can be applied to a simplified model. Attracting magnets close to the centre of rotation provide the forces for the spring (refer to Figure 4.2). Further away, *repelling* magnets are placed such that the translational forces they apply are *less* than the attractive forces of the inner magnets (see Figure 4.14(a)). However, their strengths and distances away have been carefully chosen so that the *rotational* forces (moments) they apply are *greater* than the moments applied by the inner magnets (see Figure 4.14(b)). The system may be represented by the following equations for each equal and opposite magnet pair. For the forces:

$$F_{\text{total}} = F_{\text{inner}} - F_{\text{outer}}, \quad (4.14)$$

$$F_{\text{inner}} > F_{\text{outer}}, \quad (\text{because } d > D) \quad (4.15)$$

$$\implies F_{\text{total}} > 0. \quad (4.16)$$

→ page 20

And for the moments:

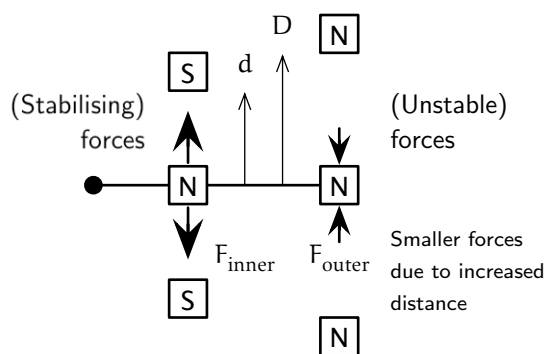
$$M_{\text{total}} = -M_{\text{inner}} + M_{\text{outer}}, \quad (4.17)$$

$$M_{\text{total}} = -rF_{\text{inner}} + RF_{\text{outer}}, \quad (4.18)$$

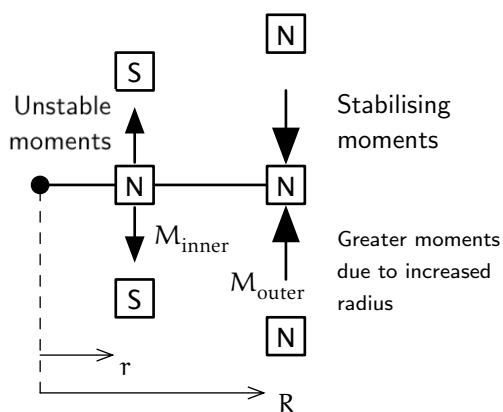
$$R \cdot F_{\text{outer}} > r \cdot F_{\text{inner}}, \quad (\text{for } M_{\text{total}} > 0) \quad (4.19)$$

$$\implies \frac{R}{r} > \frac{F_{\text{inner}}}{F_{\text{outer}}}. \quad (4.20)$$

With appropriate choices of d , D , r , and R , this condition may be satisfied. Bear in mind, of course, that $F \propto d^2$, so the ratio between r and R will need to be significantly greater than that between d and D .



(a) The added magnets are spaced farther away, so they do not affect the translational stability.



(b) The added magnets *do* affect the radial stability because their distance from the centre of rotation is much greater.

FIGURE 4.14: Secondary (outer) magnets may be added to add stability in the rotational direction.

5 Prototype considerations

This chapter covers the implementation details of the prototype spring, looking at how the forces in the spring will be estimated and secondly at the actuators and sensors that will be used. Finally, the testing plan is briefly covered.

5.1 Magnets

Magnets are required in order to build a magnetic spring! K&J Magnetics[†] is an American supplier of surplus rare earth magnets. They offer a large range of sizes, for example, from one-eighth inch cubes (100 for us\$8.20) all the way up to one inch cubes, which sell for us\$14.25 each. (These prices are very good.) For the initial stages of the project, 25 half-inch magnets were purchased from them for about us\$45. They offer bulk discounts for when many more magnets will be required in order to build up the planar arrays for the supports.

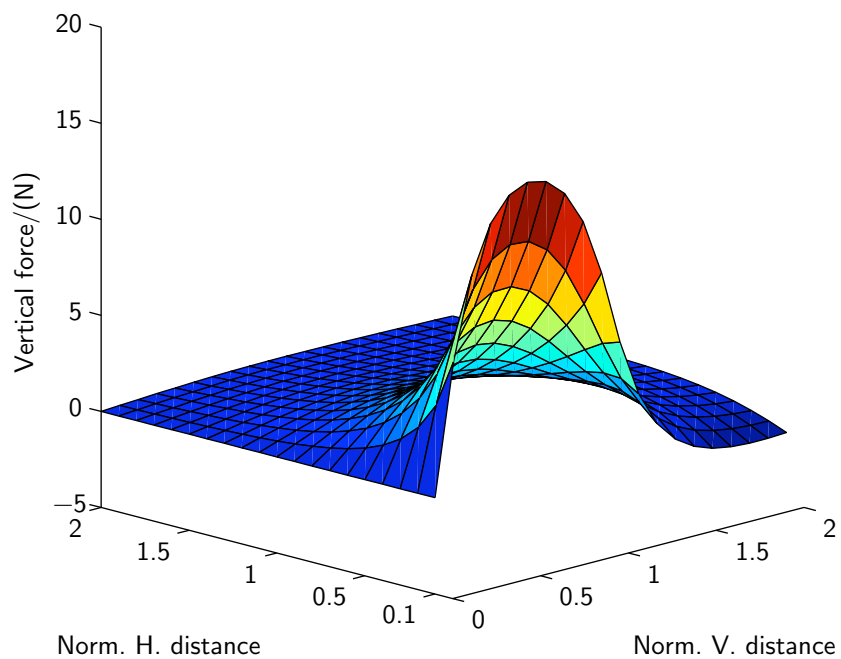
5.2 Forces between magnets

Analytical solutions to the forces that occur between arrangements of magnets are as complex as the solutions to the magnetic field—not to be undertaken lightly. It is now the trend to compute such details with FEA software rather than with elegant maths; the time-cost for the former has now decreased tremendously in recent years with increasingly-faster computers.

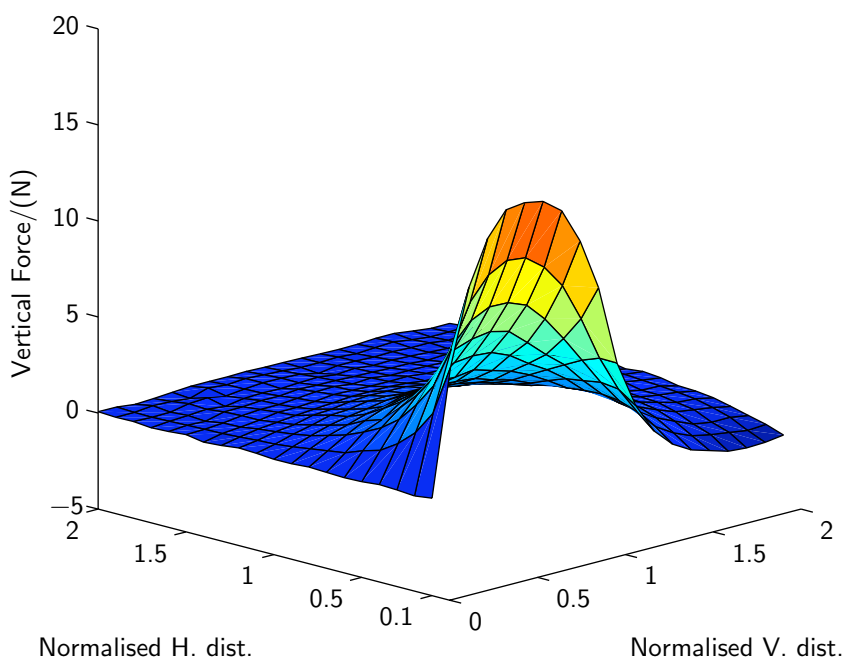
Figure 5.1 demonstrates the differences with finding the forces between two cube magnets using three techniques: analytical, as above; using FEA; and some approximate real-life measurements. The differences are quite negligible.

From these FEAREsults, curve-fit data or lookup tables may be implemented for the control system. Since the spring will be essentially motionless, the slight inaccuracies in this technique should not prove a hindrance.

[†]<http://www.kjmagnetics.com/>



(a) Analytic forces between two half-inch cube magnets.



(b) FEA forces between two half-inch cube magnets.

FIGURE 5.1: Comparison of vertical forces calculated with two methods.

5.3 Actuators

The next aspect of the prototype design involves the arrangement of the electromagnets that will be used to apply variable non-contact forces on the spring. Two separate functions are needed: stability of levitation, and rejection of vertical disturbances. These two forces are orthogonal in direction and functionality.

5.3.1 Prototype electromagnets

For the prototype spring, two sets of electromagnets have been purchased to evaluate their efficiency. Detailed measurements have been taken to determine the force/distance and force/voltage curves, since analytical information was unavailable from the supplier, Magnetech Corp.[‡]

These electromagnets are simple coil windings, with two different pole configurations: radial pole and opposite pole. The differences are determined by the pole pieces; in the former, the magnetic flux travels closer to the electromagnet's surface, but is stronger, whereas the latter has a weaker field that extends farther.

Both electromagnets are cylindrical and have the same dimensions: $\text{Ø } 1.25'' \times 1.25''$. They are designed for holding applications against one face with little or no air gap, and tests have been performed measured the force exerted by both on a steel plate. Graphs for the radial pole electromagnets can be seen in Figure 5.2.

The radial pole electromagnet has been chosen for use in this application because it outperformed the other in the tests: it has a more linear and a slightly higher force output than the opposite pole electromagnet, and it was also found that it accepts more voltage over rating without overheating.

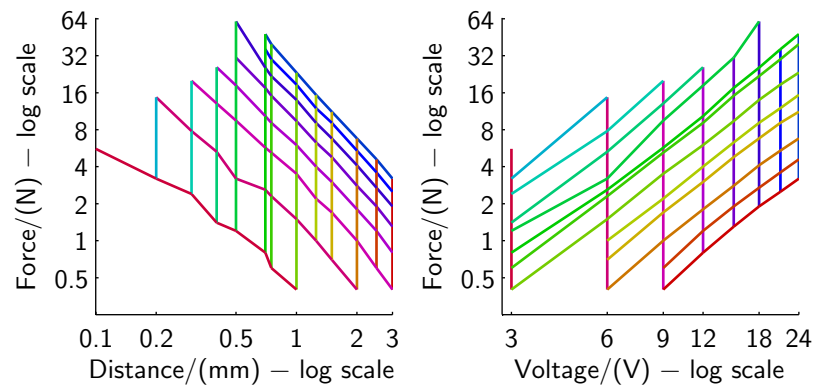


FIGURE 5.2: Performance curves of the radial pole electromagnet, rated at 12 V. Vertical lines in the distance plots define the diagonal lines in the voltage plots, and vice versa.

[‡]One of the disadvantages of a strict budget

5.3.2 Actuator placing

Initially it was thought that each individual magnetic spring could be designed to be modular such that all of the required stability and vibration isolation actuators were integrated with the permanent magnet design. However, this arrangement would ultimately lead to an inefficient table design, because each individual spring would be applying a greater control effort to the total structure compared to using a global design.

For example, in order to stabilise a single spring, as is proposed for the forthcoming prototype, four actuators are required in order to stabilise the spring: two for one linear degree of freedom, and two more to ensure stability in the angular degree of freedom in the horizontal plane.

When multiple springs are used to support an entire table, however, only four actuators again are required, since controlling the stability of the whole table will clearly also stabilise each individual spring.

Trumper *et al.* (1996) developed the electromagnetic analogue to the Halbach array: a triangular coil-winding arrangement that produces sinusoidal and predominantly single-sided flux. This technique could prove especially well suited to generating forces against permanent magnet arrays. If this electromagnetic design is used for this project, it will probably only be necessary for the final stages of the vibration isolator design.

5.4 Sensors

To keep the magnetic spring centred, it is necessary to use sensors to detect where the floating component is spatially located so that deviations may be corrected. Clearly, non-contact sensors are required for a non-contact spring. In this capacity, there are four main choices:

Ultra-sonic These sensors work by sending out modulated ultra-sonic pulses to be reflected off the target. The time spent in the round trip gives a linear indicator of the distance. Ultra-sonic sensors are cheap, but slow and inaccurate. They are unsuited for use in this project.

Inductive An inductive, or Hall effect, sensor works by exciting a coil with a high frequency AC current which induces eddy currents in the target. These eddy currents may be measured very accurately, but the whole effect is very dependent on a lack of magnetic noise. This makes these type of sensors difficult to use in magnetic applications.

Capacitive A capacitive sensor measures the capacitance between a plate and the target. It can be very accurate and quite fast. To measure large distances, however, a large capacitive head is required (approx. 1 cm diameter for every 1 mm of range.) They are also very expensive due to the conditioning electronics required.

Laser A laser sensor uses interferometry to calculate position of the target. For their price, they offer very good accuracy and speed; also, they do not suffer from electrical noise.

See Boehm *et al.* (1993) for a complete overview. At this stage in the project, monetary restrictions weigh most heavily on the choice of sensor. Several sensors suitable for this project are sold by the German company Micro-Epsilon^{††}, whose products are re-sold in Australia by Bestech^{‡‡}. A selection of commercial sensors are shown in Table 5.1.

	Sensor type		
	Laser	Capacitive	Inductive
Range (mm)	6.35	≈ 4	4
Resolution (μm)	1.9	0.4	20
Price	\$2500	\$4500	“low-cost”

TABLE 5.1: Some appropriate commercial sensors.

5.4.1 Prototype sensor

It has been possible to build a capacitive sensor in-house for the first stages of the project. The first sensor built had some small problems, mostly an issue relating to electronics noise that can be filtered out, so another is still being commissioned at the time of writing. Nonetheless, initial measurements taken with it were reasonably satisfactory and demonstrate well the approximate range and sensitivity of future models.

Figure 5.3 shows some initial calibration measurements taken with the first sensor. Against aluminium, the curves are fairly linear on a logarithmic scale. Against steel, however, the sensor did not perform as reliably; while the range is increased somewhat, the linearity is much worse. This trade-off is unacceptable, as the range increase is fairly slight when compared to the disadvantages of the inaccuracies of a linear model.

The sensor itself consists of an approximately 20 mm diameter capacitive head connected to a circuit board for signal processing. As seen from the graph, the sensor has a range of approximately 1.5 mm.

5.5 Prototypes and testing

In order to test the conceptual spring design, a number of prototypes have been conceived for a series of consecutive tests. This allows the prototype to begin

^{††}http://www.micro-epsilon.com/index_en.html

^{‡‡}<http://www.bestech.com.au/>

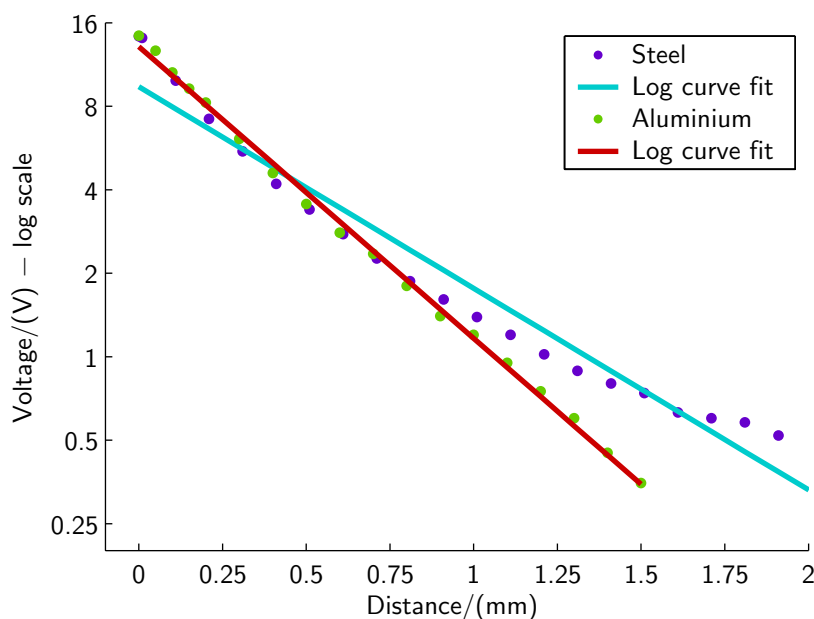


FIGURE 5.3: Calibration for the prototype capacitive sensor.

simple and become more complex as each variation is shown to work. A conceptual diagram of the prototype is shown in Figure 5.4. The stabilising magnet arrays are set up so they can be offset both horizontally and vertically from the edge of the floating spring in order to reduce the forces they apply.

The initial spring will be levitated and supported only with single cube magnets arranged horizontally as in Figure 4.2. This model will test the performance of both the sensors and the actuators. It is intended that once successful, the individual magnets will then be linked up in linear Halbach arrays, still in the horizontal configuration. Finally, the lower support magnets will be put into place and the whole system tested as a passive vibration isolator.

Once these tests are complete, a whole table can be manufactured with the final spring design, which is expected to be iteratively improved during the prototype stage. At this time vertical actuators can be included in the system and a fully active control system developed to attenuate the ground vibrations.

→ page 20

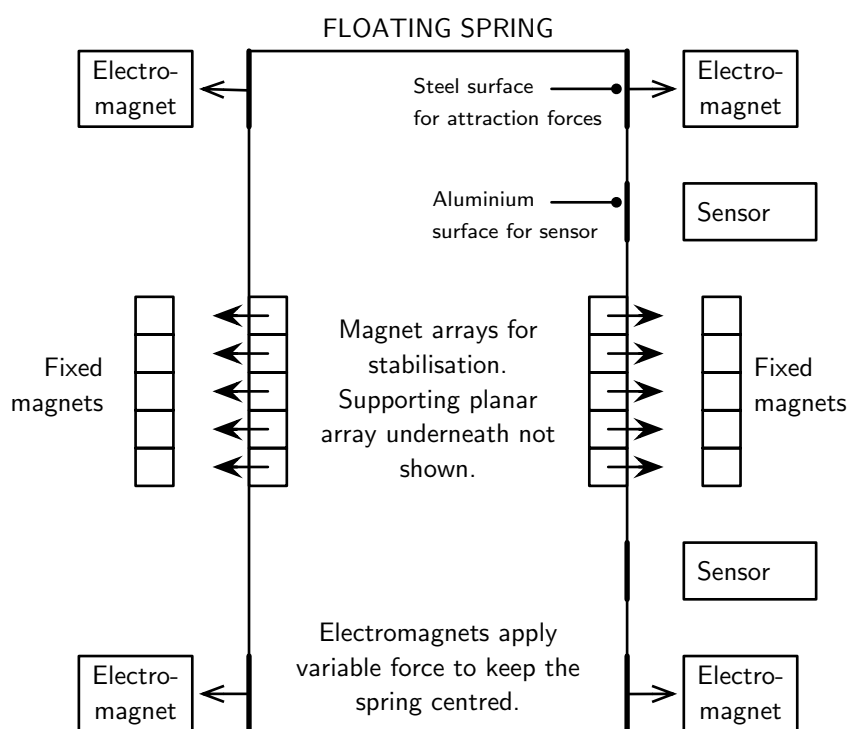


FIGURE 5.4: The prototype magnetic spring (top view).

6 Conclusions

This document summarises progress to date on a project to design a table that floats on magnets for vibration isolation. It has been shown in the literature that there have been some attempts to build a similar device, with contemporary research looking into different techniques. No current device has been built that can support large loads efficiently.

The project consists of two goals: magnetic spring design; and vibration isolator design. A basic magnetic design was shown in §4.4.5, and forces between arrays of magnets are being investigated as a way to increase the stiffness of the spring. Initial results in Figure 4.9 show that using arrays of magnets can indeed substantially increase the forces between two magnetic volumes.

→ page 29

→ page 26

6.1 Future work

Further FEA work is required to compare the more complex planar magnet arrays, followed by the physical realisation of the more promising candidates for integration into a prototype.

Work has commenced constructing a prototype spring with appropriate actuators and sensors described in Chapter 5, and testing will commence following the procedure outlined in §5.5. Two papers are anticipated in the short term: one from the planar array spring force results; the second following describing the magnetic spring design incorporating the arrays. An approximate timeline for the remainder of the project is shown in Figure 6.1.

→ page 32

→ page 36

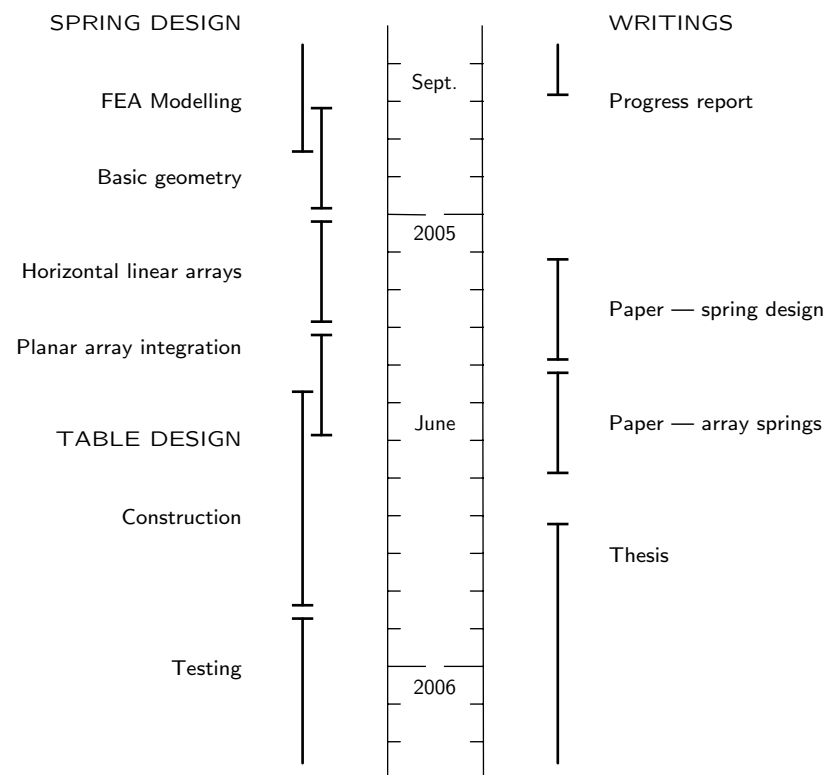


FIGURE 6.1: Approximate timeline for the rest of the project. . .

References

- AKOUN G. and YONNET J.P. (1984): 3D analytical calculation of the forces exerted between two cuboidal magnets. *IEEE Transactions on Magnetics*, MAG-20(5):1962–1964. (Cited on page 17)
- BACKERS F.T. (1961): A magnetic journal bearing. *Philips Technical Review*, 22(7):232–238. (Cited on pages vi, 6, and 9)
- BANCEL F. (1999): Magnetic nodes. *Journal of Physics D: Applied Physics*, 32:2155–2161. (Cited on page 17)
- BANCEL F. and LEMARQUAND G. (1998): Three-dimensional analytical optimisation of permanent magnets alternated structure. *IEEE Transactions on Magnetics*, 34(1):242–247. (Cited on page 9)
- BERRY M.V. and GEIM A.K. (1997): Of flying frogs and levitrons. *The European Physical Society*, 18:307–313. (Cited on page 5)
- BLEULER H. (1992): A survey of magnetic levitation and magnetic bearing types. *JSME International Journal, Series III*, 35(3):335–342. (Cited on page 6)
- BOEHM J., GERBER R. and KILEY N.R.C. (1993): Sensors for magnetic bearings. *IEEE Transactions on Magnetics*, 29(6):2962–2964. (Cited on page 36)
- BOERDIJK A.H. (1956a): Levitation by static magnetic fields. *Philips Technical Review*, 18:125–127. (Cited on pages 3 and 5)
- BOERDIJK A.H. (1956b): Technical aspects of levitation. *Philips Research Reports*, 11:45–56. (Cited on pages 4, 5, and 6)
- CAMPBELL P. (1994): *Permanent Magnet Materials and their Application*. Cambridge University Press. ISBN 0 521 56688 6. (Cited on page 13)
- CHANG S.C. (2001): Dynamics of a magnetically levitated table with hybrid magnets. *The Japan Society of Applied Physics*, 40(10):6163–6170. (Cited on page 11)
- CHO H.S., IM C.H. and JUNG H.K. (2001): Magnetic field analysis of 2-D permanent magnet array for planar motor. *IEEE Transactions on Magnetics*, 37(3):3762–3766. (Cited on pages 10, 11, 23, 27, and 28)

- CHOI K.B., CHO Y.G., SHINSHI T. and SHIMOKOHBE A. (2003): Stabilization of one degree-of-freedom control type levitation table with permanent magnet repulsive forces. *Mechatronics*, 13(6):587–603. (Cited on page 11)
- DELAMARE J., YONNET J.P. and RULLIÈRE E. (1994): A compact magnetic suspension with only one axis control. *IEEE Transactions on Magnetics*, 30(6):4746–4748. (Cited on page 29)
- EARNSHAW S. (1842): On the Nature of the Molecular Forces which regulate the Constitution of the Luminiferous Ether. *Transactions of the Cambridge Philosophical Society*, 3(1):97–112. (Cited on page 3)
- FURLANI E.P. (1993): A formula for the levitation force between magnetic disks. *IEEE Transactions on Magnetics*, 29(6):4165–4169. (Cited on page 17)
- HALBACH K. (1980): Design of permanent multipole magnets with oriented rare earth cobalt material. *Nuclear Instruments and Methods*, 169(1):1–10. (Cited on page 9)
- HALBACH K. (1981): Physical and optical properties of rare earth cobalt magnets. *Nuclear Instruments and Methods*, 187:109–117. (Cited on page 9)
- HOBURG J.F. (2004): Modeling maglev passenger compartment static magnetic fields from linear halbach permanent magnet arrays. *IEEE Transactions on Magnetics*, 37(5):59–64. (Cited on page 9)
- KIM W.J. (1997): *High-Precision Planar Magnetic Levitation*. Ph.D. thesis, Massachusetts Institute of Technology. (Cited on pages 8, 10, 23, 25, and 28)
- LAITHWAITE E.R. (1965): Electromagnetic levitation. *Proceedings of the Institution of Electrical Engineers*, 112(12):2361–2375. (Cited on page 5)
- MA K.B., POSTREKHIN Y.V. and CHU W.K. (2003): Superconductor and magnet levitation devices. *Review of Scientific Instruments*, 74(12):4989–5017. (Cited on page 5)
- MIZUNO T., SUZUKI H. and TAKASAKI M. (2003a): Development of an active vibration isolation system using zero-power magnetic suspension. In *Tenth International Congress on Sound and Vibration*, pages 887–894. Stockholm, Sweden. (Cited on page 11)
- MIZUNO T., SUZUKI H., TAKASAKI M. and ISHINO Y. (2003b): Development of a three-axis active vibration isolation system using zero-power magnetic suspension. In *Proceedings of the 42nd IEEE Conference on Decision and Control*, pages 4493–4498. Maui, Hawaii USA. (Cited on page 11)

- MOLENAAR L. (2000): *A novel Planar Magnetic Bearing and Motor Configuration applied in a Positioning Stage*. Ph.D. thesis, Department of Mechanical Engineering and Marine Technology, Delft University of Technology, the Netherlands. (Cited on page 8)
- MOSKOWITZ L.R. (1995): *Permanent Magnet Design and Application Handbook*. Kreiger Publishing Company, Kreiger Drive, Malabar, Florida 32950, second edition. ISBN 0-89464-768-7. (Cited on page 16)
- NAGAYA K., ATSUMI M. and ENDOH M. (1993): Simplified vibration isolation control using disturbance cancellation and velocity feedback controls for a magnetic levitation table. *International Journal of Applied Electromagnetics in Materials* 4, 4(4):115–122. (Cited on page 10)
- NAGAYA K. and ISHIKAWA M. (1995): A noncontact permanent magnet levitation table with electromagnetic control and its vibration isolation method using direct disturbance cancellation combining optimal regulators. *IEEE Transactions on Magnetics*, 31(1):885–895. (Cited on page 10)
- PUPPIN E. and FRATELLO V. (2002): Vibration isolation with magnet springs. *Review of Scientific Instruments*, 73(11):4034–4036. (Cited on page 10)
- SIMON M.D. and GEIM A.K. (2000): Diamagnetic levitation: Flying frogs and floating magnets. *Journal of Applied Physics*, 87(9):6200–6204. (Cited on page 5)
- SIMON M.D., HEFLINGER L.O. and GEIM A.K. (2001): Diamagnetically stabilized magnet levitation. *American Journal of Physics*, 69(6):702–713. (Cited on page 5)
- TONKS L. (1940): Note on Earnshaw's Theorem. *Electrical Engineering*, 59(3):118–119. (Cited on page 3)
- TRUMPER D.L., KIM W.J. and WILLIAMS M.E. (1996): Design and analysis framework for linear permanent-magnet machines. *IEEE Transactions on Industry Applications*, 32(2):371–379. (Cited on page 35)
- TRUMPER D.L. and QUEEN M.A. (1992): Control and actuator design for a precision magnetic suspension linear bearing. In *Controls for Optical Systems*, volume 1696 of *Proceedings of SPIE - The International Society for Optical Engineering*, pages 2–15. Orlando, FL, USA. (Cited on page 8)
- VERMA S., KIM W.J. and GU J. (2004): Six-axis nanopositioning device with precision magnetic levitation technology. *IEEE/ASME Transactions on Mechatronics*, 9(2):384–391. (Cited on page 8)
- VISCHER D. and BLEULER H. (1993): Self-sensing active magnetic levitation. *IEEE Transactions on Magnetics*, 29(3):1276–1281. (Cited on page 6)

- WATANABE K., HARA S., KANEMITSU Y., HAGA T., YANO K., MIZUNO T. and KATAMURE R. (1996): Combination of h^∞ and pi control for an electromagnetically levitated vibration isolation system. In *Proceedings of the 35th IEEE Conference on Decision and Control*, volume 2, pages 1223–1228. (Cited on page 10)
- YONNET J.P. (1978): Passive magnetic bearings with permanent magnets. *IEEE Transactions in Magnetism*, MAG-14(5):803–805. (Cited on page 6)
- YONNET J.P. (1981): Permanent magnet bearings and couplings. *IEEE Transactions on Magnetism*, MAG-17(1):1169–1173. (Cited on pages 8 and 20)
- YONNET J.P., LEMARQUAND G., HEMMERLIN S. and OLIVIER-RULLIERE E. (1991): Stacked structures of passive magnetic bearings. *Journal of Applied Physics*, 70(10):6633–6635. (Cited on pages 9 and 22)